

Finite-Element Analysis and Design of a Radial-Field Brushless PM Machine Utilizing Soft Magnetic Composites

G.S. Liew, C. Tang, W.L. Soong and N. Ertugrul
University of Adelaide, Australia
Email: gliew@eleceng.adelaide.edu.au

D.B. Gehlert
Intelligent Electric Motor Solutions Pty. Ltd., Australia
Email: davidg@diga.com.au

Abstract—Soft magnetic composites (SMC) are emerging in electrical machine design offering the potential for innovative machine geometries and lower cost manufacturing. This paper examines the design and analysis of a SMC-based radial-field fractional-slot concentrated-winding permanent magnet machine using 2D finite-element analysis. Its performance is compared with an existing conventionally-laminated, distributed-winding baseline design for two cases, firstly with the same active stack length and secondly with the same end-winding stack length.

I. INTRODUCTION

The use of soft magnetic composites (SMC) in electrical machines offers the potential for simplified and lower cost manufacturing methods, innovative 3D machine design topologies, higher power density, and better winding utilization [1], [2]. SMC is manufactured from iron powder coated with a small amount of binder. It can be pressed into 3D core shapes with its magnetic properties depending on the binder and pressure used. It generally has low eddy current losses due to its high resistivity, but it has relatively low permeability, low mechanical strength, and high hysteresis losses compared to silicon-iron based laminated core structures.

This paper describes the design of an optimised SMC surface permanent magnet (PM) machine based on the specification and dimensions of an existing conventionally laminated baseline machine. The key requirements are low cogging torque and high power density with a rated speed of 1,000rpm, total stack length of less than 50mm (including end-turns) and an outer diameter of 134mm.

The baseline machine has a distributed-winding with 36 slots and 12 poles, a short (14mm) magnetic stack length (50mm overall stack length) and uses conventional laminations and sintered neodymium magnets. This paper investigates a SMC based fractional-slot concentrated-winding machine using 2D finite-element (FE) analysis. A SMC concentrated-winding machine with an identical active stack length (14mm) is modeled initially. Next, a higher power SMC machine design with a longer active stack length but the same total stack length (including end-windings) of 50mm is investigated using bonded instead of sintered neodymium magnets. This uses the 3D design capability of SMC to allow the stator tooth tips and yoke to have the same axial length as the stator winding, producing “internal” end-windings. A custom-built

die was used to mould the SMC teeth in order to construct a prototype to validate the design and FE model. In this paper, the design and optimisation of the two different stack length SMC machines is reported.

II. 14MM STACK LENGTH DESIGN WITH SINTERED NEODYMIUM MAGNET AND EXTERNAL END-WINDINGS

The baseline model (base model) is a distributed-winding design which has a relatively large end-winding copper loss due to its short stack length. It uses magnets which are skewed (non-uniform spacing) and have a tapered airgap surface to give low cogging torque. Figure 1(a) shows the cross-sectional drawing of the baseline model. Also in Figure 1 are the cross-sections of two 14mm and one 50mm active stack length SMC designs, note the dimension shown in the figures is the overall axial length.

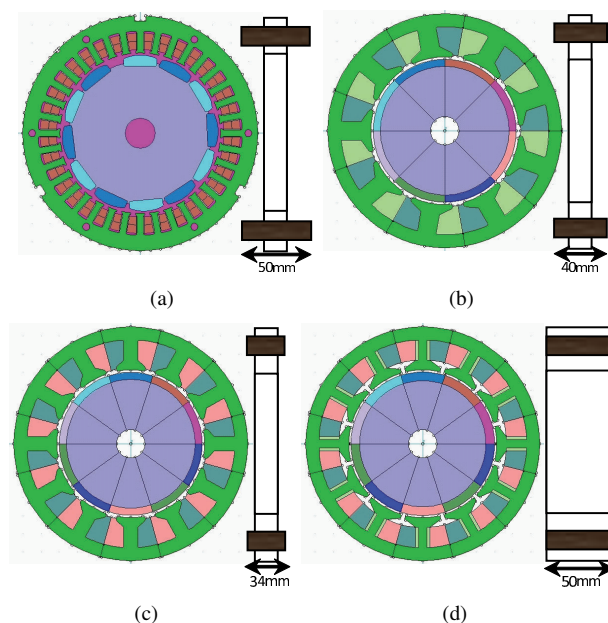


Fig. 1. Radial and axial views showing the total stack length of: a) base model, b) SMC 9S8P, c) SMC 12S10P and d) SMC 12S10P 50mm, stack length with internal winding.

The number of slots was chosen as a trade-off between the difficulty of assembling numerous moulded teeth and the desire for a relatively high number of poles to minimise end-winding and yoke thickness. According to [3], [4], fractional-slot configurations with a numbers of stator slot per pole q between 0.33 and 0.5 generally have good performance and low cogging torque. Therefore, the 9 slot 8 pole (9S8P, see Figure 1(b)) and 12 slot 10 pole (12S10P, see Figure 1(c)) were considered. A stator copper packing factor (copper area/total slot area) for the fractional-slot windings of 45% was assumed. The key parameters of the motors are given in TABLE I.

TABLE I
KEY PARAMETERS OF THE 14 MM ACTIVE STACK-LENGTH MODELS.

Parameter	Base Model (Distributed)	SMC 9S8P (Concentrated)	SMC 12S10P (Concentrated)
Stator Material	Polycor	SMC	SMC
-Outer Diameter	134mm	134mm	134mm
-Inner Diameter	91mm	84.4mm	84.4mm
-Stack Length	14mm	14mm	14mm
Stator tooth ratio t	0.37	0.29	0.29
Number of Slots	36	9	12
Number of Poles	12	8	10
Airgap Length	1.2mm	1.41mm	1.41mm
Magnet Remanent Flux Density, B_R	1.11T	1.05T	1.05T
Magnet Thickness	6.35mm (Peak Arc)	4mm (Ring)	4mm (Ring)
Winding Factor	1	0.945	0.966
End-turn Length	18mm	13mm	10mm

A. 2D FEA Results

Finite-element analysis is a numerical method that can accurately analyze complex electromagnetic fields using Maxwell's equations. In this work, the finite-element package "JMAG-studio" (JMAG) [5] was employed as the design tool to simulate and to predict the characteristics of the motor. An identical stator tooth ratio t (tooth width/tooth pitch) of 0.29 (discussed later) was applied to the 9S8P and 12S10P configurations and hence a comparable iron weight is obtained. The output torque and iron loss were generated from the FE model while the stator copper loss was calculated from the current density J , electrical resistivity of the copper and the volume of the copper including the estimated end-windings. For the base distributed-winding machine model, the measured resistance was used to estimate the copper loss based on the simulated current at certain torque value.

Figure 2 compares the calculated losses of the baseline machine with the 9 slot and 12 slot SMC designs with the same active stack length (14mm) at the rated torque of 3Nm and 1,000rpm. It shows the calculated slot copper, end-winding copper, stator iron, magnet and rotor eddy-current loss. The copper loss, and in particular, the end-winding copper loss is the dominant loss due to the short stack-length and low rated speed. In the base machine the end winding copper loss is over eight times higher than the slot copper loss. The two fractional-slot SMC machines have less than half the end-winding copper loss and total copper losses compared to the base model. The stator slot copper loss of the base machine is 25% lower than

the fractional-slot designs. This is partly due to the slightly smaller winding factor and magnet remanent flux density of the fractional-slot designs.

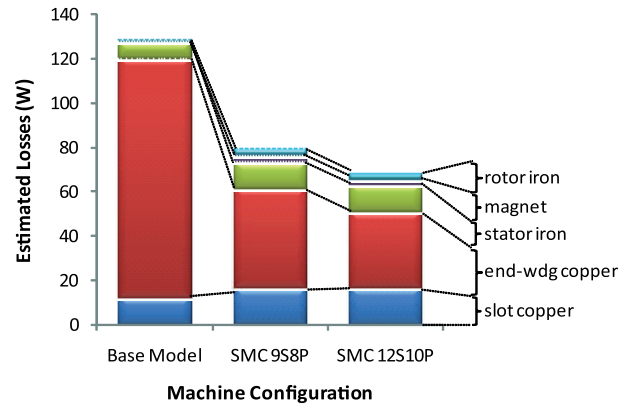


Fig. 2. 14mm active stack length machines at the rated torque of 3Nm and 1,000rpm. Calculated slot copper, end-winding copper, stator iron, magnet and rotor eddy-current loss.

Figure 2 shows that the iron loss in the base model is relatively small due to the low rated speed. The iron loss approximately doubles for the SMC designs, due to the higher loss of the SMC material. In addition, the magnet and rotor back-iron eddy-current loss is small for the distributed base model but significantly higher for the SMC designs due to the larger amplitude, higher harmonics produced by the fractional-slot winding. This is not an issue at the low design speed but would be more important at high speeds.

Figure 3 shows the calculated efficiency versus torque characteristics of the three machines at 1,000rpm. The base model has lower iron losses and so is expected to have higher efficiency at light loads. At high loads, the fractional-slot designs have significantly higher efficiency due to their lower copper loss. For instance at the rated torque of 3Nm, about 10% higher efficiency is predicted for the fractional-slot designs.

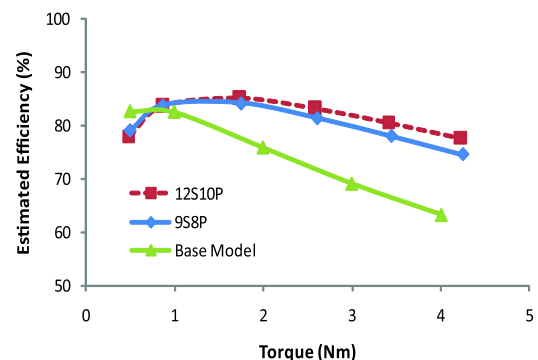


Fig. 3. 14mm active stack length machines, calculated efficiency versus torque at 1,000rpm.

Figure 4 gives the simulated peak cogging torques for

the three machines as a function of eccentricity. With zero eccentricity, the cogging torque for all three models are less than 0.5% of rated torque (3Nm). The base model achieved this using skewed magnets and shaped magnet poles however neither of these measures were required in the fractional-slot designs. The figure also shows the sensitivity of the cogging torque to eccentricity. With 25% eccentricity, the calculated cogging torque of the base model and the 12S10P machine increases to about 1% while for the 9S8P machine the cogging torque increases to 2.5% of the rated torque. Therefore, the 12S10P was chosen as low cogging torque design.

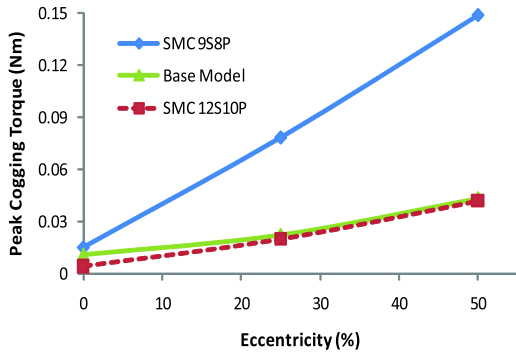


Fig. 4. 14mm active stack length machines, calculated peak cogging torque versus eccentricity.

The optimisation of the SMC machine tooth ratio (tooth width to tooth pitch) was also considered. Figure 5 shows the copper and total loss at rated torque as a function of tooth width ratio. The iron loss is relatively small at the low rated speed and so the total loss is dominated by the copper loss. Reducing the tooth width increases the slot area and hence reduces the stator resistance. Thus starting with high values of tooth ratio, the copper loss initially falls as the tooth ratio is decreased. However at low values of tooth width, the teeth start to saturate which reduces the back-emf voltage and thus increases the required current to achieve rated torque. This effect causes the copper loss to reach a minimum (in this case, with a ratio of 0.29) before increasing again. This “optimum” tooth ratio was used in the two 14mm stack-length SMC designs.

III. 50MM STACK LENGTH DESIGN WITH BONDED NEODYMIUM MAGNET AND INTERNAL END-WINDINGS

A. Equivalent 2D FE Model

The next part of this study is to design a 50mm fractional-slot SMC machine with the same total axial length including end-windings as the baseline machine. In order to simplify the rotor construction and to limit the magnet eddy-current losses, the design was based on bonded neodymium magnets. This uses the 3D capability of SMC to produce “internal” end-windings. Note the machine has considerably more iron than the original machine (though a comparable amount of copper) and should be capable of substantially higher output power.

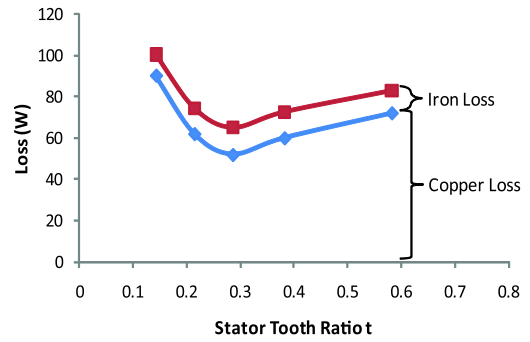


Fig. 5. 14mm stack length 12S10P SMC design. Estimated copper and iron loss plot at $T = 3\text{Nm}$ and 1,000rpm as a function of tooth ratio.

As 3D FE analysis is complex and time consuming, an equivalent 2D FE model using a narrower “effective” tooth width is used (see Figure 1(d)) as demonstrated in [6]. The 2D FE models use a stack length equal to the original tooth and yoke length but narrower tooth body width to give it the same tooth body cross-sectional area as the actual machine. The simulation results are from a time-stepping, coupled-circuit 2D finite element simulation. The mesh of the models consists of 21,900 nodes and 37,600 elements. The BH-curves and iron loss characteristics available in the JMAG material database for the Somaloy 550 + 0.5% Kenolube was used. The total execution time was approximately 8 minutes for 180 steps.

For the final design of the 50mm SMC model, the tooth tip opening was set at 2mm to provide more mechanical support for the winding. This would also reduce the cogging torque. In addition, the same 45% winding packing factor as the 14mm stack length design was assumed in the analysis. The design and optimization of this machine is discussed in the following sections.

B. Optimisation of the Stator Slot Ratio

In this section, the stator slot ratio of the 50mm stack length machine was optimised by changing the tooth body length (TBL). The axial width of the stator coil is half the difference between the stack length(50mm) and the tooth body length. As the tooth body length is reduced, the tooth body width must be adjusted to allow sufficient room for the winding in the stator slot.

Figure 6 shows the machine cross-sections with four different values of stator slot ratio obtained by changing the tooth body length and width. Bonded magnets of $B_R = 0.6\text{T}$ and 5mm thickness were selected. Figures 6(a) and 6(d) demonstrate extreme cases taking into consideration the physical limitations of the stator poles and slot width and the other two cases are intermediate examples. Note that in the 2D FE models, the tooth body width is reduced below its actual value to compensate for the fact that the tooth body length is shorter than the stack length.

Table II gives the calculated stator iron and copper weights based on the densities of the materials, and also the simulated

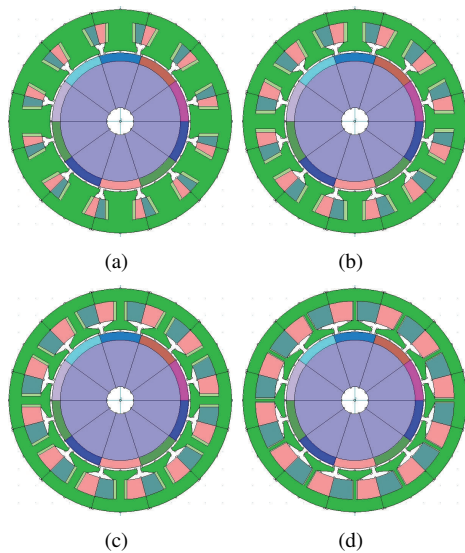


Fig. 6. 50mm stack-length 12S10P SMC designs with different tooth body lengths (stator tooth ratios), a) 40mm, b) 35mm, c) 30mm and d) 25mm.

peak cogging torque. The magnitude of the peak cogging torque falls from about 2.5% to about 1% of rated torque with decreasing tooth body length.

TABLE II

50MM MACHINE. OPTIMISATION OF STATOR SLOT RATIO. WEIGHTS AND PEAK COGGING TORQUE FOR DIFFERENT TOOTH BODY LENGTH.

	Stator Weight (kg)	Copper Weight (kg)	Peak Cogging Torque (Nm)
TBL40	2.29	0.45	0.076
TBL35	1.98	0.61	0.068
TBL30	1.73	0.78	0.037
TBL25	1.54	0.86	0.026

Figure 7 shows the back-emf waveforms for the four designs. With high values of tooth body length (and hence the iron area) the back-emf waveform is relatively constant, however particularly for the smallest tooth body length considered, the stator teeth saturate which substantially reduces the back-emf voltage magnitude.

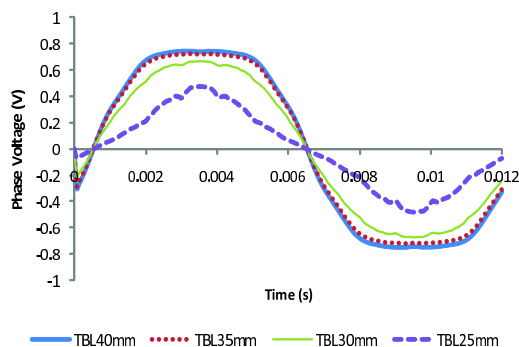


Fig. 7. Phase back-EMF waveforms for four 50mm SMC designs with varying tooth body length. Based on one turn per coil at 1,000rpm.

Figure 8 shows the calculated loss breakdown at the rated torque of 3Nm and 1,000rpm for the four designs. The variation of the total copper loss and iron loss as a function of tooth body length is shown in Figure 9. The minimum total loss under rated conditions is obtained with the 30mm tooth body length, which corresponds to a stator tooth ratio of about 0.3. This is consistent with what was found for the 14mm active stack length designs (see Figure 5).

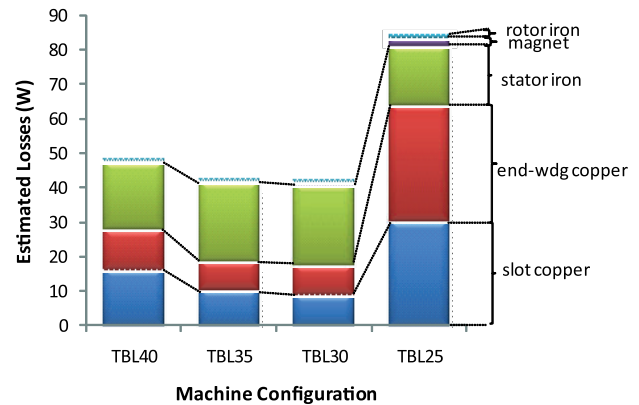


Fig. 8. Four 50mm SMC designs with varying tooth body length. Calculated slot copper, end-winding copper, stator iron, magnet and rotor eddy-current loss at the rated torque of 3Nm and 1,000rpm.

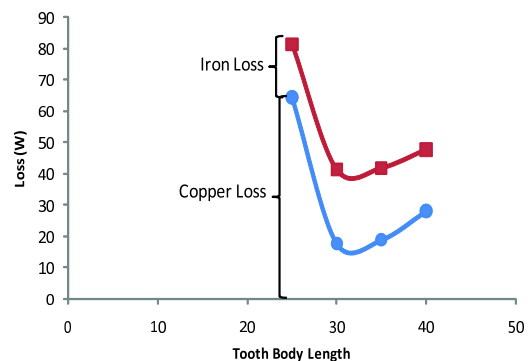


Fig. 9. Estimated copper and iron loss plot at $T = 3\text{Nm}$ and 1,000rpm for the 50mm 12S10P SMC design as a function of tooth body length.

Reducing the tooth body length below the optimum value of 30mm causes stator tooth saturation, the back-emf to fall, the required stator current to increase and the stator copper losses to dramatically increase. Increasing the tooth body length above 30mm causes a slight decrease in the iron loss due to the lower stator flux densities, however this is offset by the stator copper losses increase due to the reduction of copper area.

Figure 10 shows the estimated efficiency versus torque curves for the four designs with different stator tooth body lengths at 1,000rpm. The designs with tooth body lengths of 30mm and 35mm have the highest efficiency when operating above 2Nm. The 40mm tooth body length design has slightly

higher efficiency for torques in the range of 1 to 2Nm. The efficiency of the 25mm tooth body length design drops substantially at higher torques due to the high copper loss.

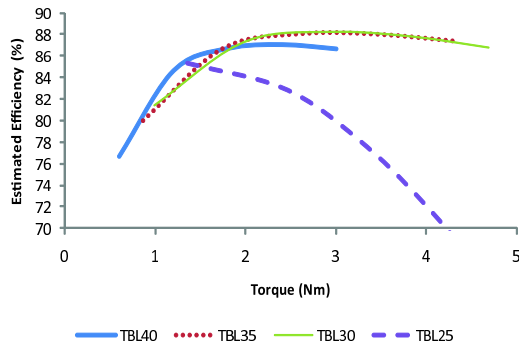


Fig. 10. Calculated efficiency versus torque curves at 1,000rpm for the four 50mm SMC designs with different tooth body lengths.

IV. COMPARISON OF THE BASELINE AND 14MM/50MM SMC DESIGNS

This section provides a comparison of the baseline machine with the two optimised SMC designs, one with the same active stack length (14mm) and the other with the same total stack length (50mm). Table III summarises the key parameters for the three machines.

TABLE III
KEY PARAMETERS OF THE MODELS.

Parameter	Base Model	SMC (14mm)	SMC (50mm)
Winding Configuration	Distributed (external end)	Concentrated (external end)	Concentrated (internal end)
Packing factor	0.45	0.45	0.45/0.30
Stack Length			
- Total	50mm	25mm	50mm
- Stator	14mm	14mm	50mm
- Tooth Body	14mm	14mm	30mm
Neodymium Magnet	Sintered	Sintered	Bonded
B_R (T)	1.11T	1.05T	0.6T
Thickness	6.35mm	4mm	5mm

It had been assumed that the SMC designs with concentrated-windings could achieve a 45% copper packing factor. Experimentation with winding the stator cores showed that this is just possible with careful winding, however the windings used in the prototype unit had only a modest 30% packing factor.

Figure 11 gives the weight comparison of the baseline machine, the 14mm SMC design and the 50mm SMC design with two different copper packing factors. For the baseline and 14mm SMC machines, the stator weight is comparable but the copper required is estimated to be 50% less for the SMC design due to the smaller end-windings. As for the 50mm SMC machines, about three times more SMC material is utilised and about 40% more copper is required compared to the 14mm SMC design. In addition, it uses three times magnet material (bonded rather than sintered magnets).

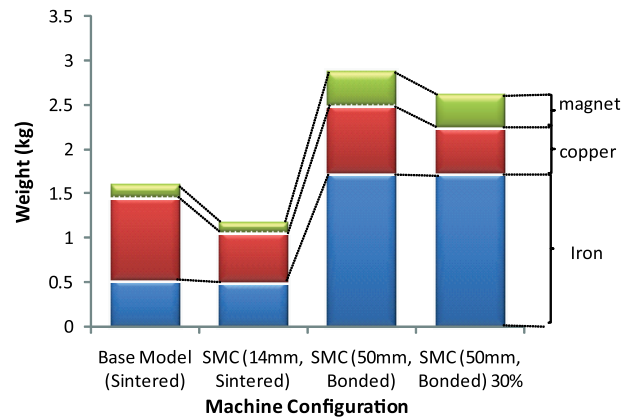


Fig. 11. Estimated stator iron, copper and magnet weight of the baseline machine, the 14mm SMC design and the 50mm SMC design with two copper packing factors.

Figure 12 shows the calculated efficiency plot of the four machine designs as a function of torque. As it was seen earlier in Figure 3, the efficiency of the baseline design drops rapidly as the torque is increased due to its high copper losses. The 14mm SMC design shows a significant efficiency improvement above 1Nm. The 50mm SMC design maintains high efficiency at higher torques, however when its packing factor is reduced from 45% to 30% its performance drops and becomes comparable to the 14mm SMC design.

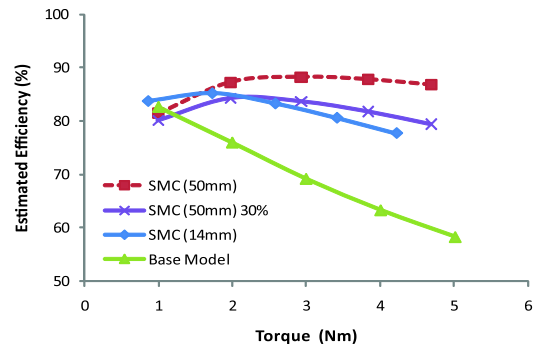


Fig. 12. Calculated efficiency versus torque at 1,000rpm for the four machine designs shown in Figure 11.

Figure 13 shows the loss breakdown for the four machine designs for torque of 3Nm and at 1,000rpm. The end-winding copper loss drops substantially from being the dominant loss in the baseline design to being about a quarter of the total losses in the 50mm SMC designs. This is due to the shorter end-windings of the concentrated-winding SMC designs and the reduced stator current density due to the longer stack-length. On the other hand, the stator iron losses increase when moving from left to right. The 14mm SMC design has about twice the iron loss of the baseline design due to the higher loss density in SMC, and the 50mm SMC designs have about twice the iron loss of the 14mm SMC design due to the greater

amount of iron in the machine. The 14mm SMC design shows a significant magnet and rotor iron eddy-current loss due to its fractional-slot arrangement with sintered magnets, however the bonded magnets used in the 50mm design mean that these losses are negligible.

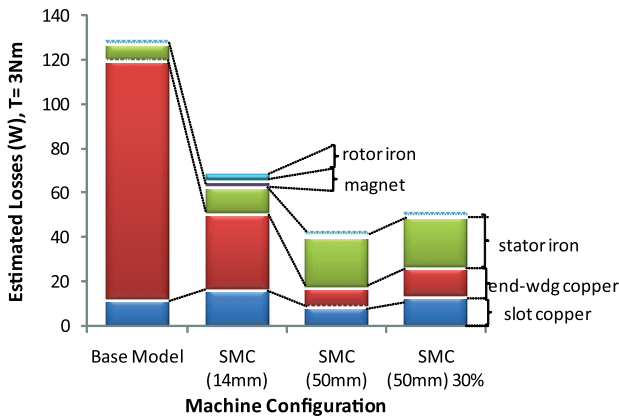


Fig. 13. Calculated slot copper, end-winding copper, stator iron, magnet and rotor eddy-current loss at the torque of 3Nm and 1,000rpm for the four designs in Figure 11.

V. PROTOTYPE 50MM SMC PM MOTOR

A precision, custom-built die was constructed to produce the SMC stator poles. This approach gives much better dimensional tolerances and surface finish than can be achieved by machining. A modest 30% packing factor was achieved by manually winding the prototype pole pieces utilizing three strands of wires, though some experimentation showed that 45% is just possible. Note that the packing factor definition used here is the area of the copper divided by the total slot area.

The housing for the prototype is presently being constructed. After the assembly of the prototype machine, a comprehensive series of tests will be conducted to validate the accuracy of the model considered (12S10P).

VI. CONCLUSION

This paper presents a detailed finite-element (FE) based design study of a fractional-slot concentrated-winding surface PM motor utilizing soft magnetic composites (SMC) based on the specification and size of a baseline conventionally-laminated distributed-winding machine. The use of a 3D SMC stator allows better winding utilization and higher power density.

Firstly, an identical active stack length (14mm) SMC design was modeled. Both the 9 slot 8 pole and 12 slot 10 pole configurations were investigated. The 12 slot design was selected as it had slightly higher efficiency and a lower value of cogging torque which was less sensitive to eccentricity. The concentrated-winding SMC design showed substantially lower end-winding copper loss but somewhat higher slot copper

losses and iron losses. Its total losses at rated output was approximately half that of the baseline design.

Secondly, an identical total stack length (50mm) SMC design was modeled which used a 3D stator core arrangement with stator end-windings being enclosed by the stator teeth. The longer stack length meant that the amount of iron in the design increased by a factor of three. To simplify construction, bonded magnets were used rather than the sintered magnets used in the baseline and 14mm SMC designs. This longer stack length design had even lower copper losses than the 14mm SMC design and produced a total loss at rated output which was approximately one third that of the baseline design. It showed the capability to maintain high efficiency at high output torques.

For both the 14mm SMC design with sintered magnets, and the 50mm SMC design with bonded magnets and 3D teeth, it was found that a 30% ratio between the width of the stator tooth body and the stator tooth pitch minimised the total loss at the rated torque and speed considered.

For the above SMC designs, a 45% copper packing factor was assumed. Experimentation using the die-case teeth showed this was just possible to achieve, though the 50mm SMC prototype unit used windings with a modest 30% packing factor. This lower packing factor will cause a significant increase in copper losses at high torque values. The prototype machine is presently being assembled and after this is complete, an extensive series of tests will be performed to validate the FE model predictions.

ACKNOWLEDGMENT

The authors would like to thank the staff of Intelligent Electric Motor Solutions Pty. Ltd. for manufacturing the machine components and the School of Electrical and Electronic Engineering mechanical workshop for their help in assembling the prototype.

REFERENCES

- [1] L. Hultman and A. Jack, "Soft magnetic composites - motor design issues and applications," in *Powder Metallurgy and Particulate Materials PM2TEC*, Chicago, USA, June 2004.
- [2] M. Persson, G. Nord, L. Pennander, G. Atkinson, and A. Jack, "Development of somaloy components for a bldc motor in a scroll compressor application," in *Powder Metallurgy PM World Congress & Exhibition*, Busan, Korea, September 2006.
- [3] J. Cros and P. Viarouge, "Synthesis of high performance PM motors with concentrated windings," *IEEE Transactions on Energy Conversion*, vol. 17-2, pp. 248-253, June 2002.
- [4] D. Ishak, Z. Zhu, and D. Howe, "Permanent-magnet brushless machines with unequal tooth widths and similar slot and pole numbers," *IEEE Transactions on Industry Applications*, vol. 41, no. 2, pp. 584-590, March 2005.
- [5] JRI Solutions, Limited, "JMAG-Studio 10.0 User's Manual Pre/Post (english version)," Web, 2011, <http://www.jri.co.jp/pro-eng/jmag/e/jmg/> Last Checked: February 21 2011.
- [6] G. Liew, N. Ertugrul, W. Soong, D. Atkinson, and D. Gehlert, "Analysis of a segmented brushless pm machine utilising soft magnetic composites," in *IEEE Industrial Electronics Society (IECON)*, Taipei, Taiwan, November 2007.